



Review

Fiber Optic Fiber Bragg Grating Sensing for Monitoring and Testing of Electric Machinery: Current State of the Art and Outlook

Asep Andi Suryandi ¹, Nur Sarma ², Anees Mohammed ³, Vidyadhar Peesapati ¹ and Siniša Djurović ^{1,*}

¹ Department of Electrical and Electronic Engineering, School of Engineering, The University of Manchester, Manchester M13 9PL, UK

² Department of Engineering, Durham University, Durham DH1 3LE, UK

³ Department of Engineering, University of Benghazi, Benghazi 3332+MV4, Libya

* Correspondence: sinisa.durovic@manchester.ac.uk

Abstract: This paper presents a review of the recent trends and the current state of the art in the application of fiber optic fiber Bragg gratings (FBG) sensing technology to condition the monitoring (CM) and testing of practical electric machinery and the associated power equipment. FBG technology has received considerable interest in this field in recent years, with research demonstrating that the flexible, multi-physical, and electromagnetic interference (EMI) immune in situ sensing of a multitude of physical measurands of CM interest is possible and cannot be obtained through conventional sensing means. The unique FBG sensing ability has the potential to unlock many of the electric machine CM and design validation restrictions imposed by the limitations of conventional sensing techniques but needs further research to attain wider adoption. This paper first presents the fundamental principles of FBG sensing. This is followed by a description of recent FBG sensing techniques proposed for electric machinery and associated power equipment and a discussion of their individual benefits and limitations. Finally, an outlook for the further application of this technique is presented. The underlying intention is for the review to provide an up-to-date overview of the state of the art in this area and inform future developments in FBG sensing in electric machinery.

Keywords: fiber Bragg grating (FBG); fiber optic sensors; electric machines; drives; high voltage assets; condition monitoring; fault detection; in situ sensing



Citation: Suryandi, A.A.; Sarma, N.; Mohammed, A.; Peesapati, V.; Djurović, S. Fiber Optic Fiber Bragg Grating Sensing for Monitoring and Testing of Electric Machinery: Current State of the Art and Outlook. *Machines* **2022**, *10*, 1103. <https://doi.org/10.3390/machines10111103>

Academic Editors: Khandaker Noman, Anil Kumar, Shah Limon and Yongbo Li

Received: 29 October 2022

Accepted: 17 November 2022

Published: 21 November 2022

Publisher's Note: MDPI stays neutral with regard to jurisdictional claims in published maps and institutional affiliations.



Copyright: © 2022 by the authors. Licensee MDPI, Basel, Switzerland. This article is an open access article distributed under the terms and conditions of the Creative Commons Attribution (CC BY) license (<https://creativecommons.org/licenses/by/4.0/>).

1. Introduction

The condition monitoring of electrical machinery is progressively gaining importance as the utilization of electric machines is increasing at an unprecedented scale, driven considerably by the proliferation of renewable power generation, transport electrification, and the ongoing automation of industrial processes [1,2]. Conventional condition monitoring (CM) methods for electrical machines have significant limitations in providing the levels of diagnostic reliability required for maintaining future mission-critical machine applications in service. This primarily concerns the delivery of a diagnosis that can allow for the prevention or minimization of costly and unnecessary outages (e.g., wind turbine generators), as well as the reduction in any related safety concerns in specific demanding applications (e.g., electric propulsion).

It is generally desirable in practical applications for CM systems to be as non-invasive as possible: this can often contradict the aim of reliable diagnosis, which largely depends on sensing access to key localized physical measurands that optimally characterize a particular failure process (e.g., heat, strain, etc.). Conventional CM is not optimally suited to this, as it relies heavily on the analysis of diagnostic data collected through the application of limited sensing devices that are frequently not optimally placed to capture or characterize a localized fault process. This is particularly valid where sensing implementation in locations

within the electric machine geometry is concerned. In situ sensing in the vicinity of known failure points or in known stress areas, could yield a much better understanding and monitoring of critical diagnostic measurements. This could, in turn, enable a much-improved characterization of the fault process inception and its propagation stages to ultimately yield an improved reliability diagnosis [3–5]. The availability of such in situ sensing abilities would not only enable better diagnostics but would be of use in machine design and prototyping stages for the high fidelity characterization of the device operating performance envelope and make it possible to improve the machine design process and perform a more thorough evaluation of machine stress and performance models [6,7]. Neither of these can be supported by the conventional sensing that is commonly employed in standard electric machine CM schemes, where sensing limitations can prevent the better utilization of CM for a more reliable and timely diagnosis [2,8,9]. There is, therefore, a significant amount of interest in the development of multi-physical embedded sensing alternatives for electric machine CMs, including the observation of a range of multi-physical parameters (e.g., thermal, strain, flux, etc.) to permit the advanced monitoring and understanding of essential stress measurands.

Fiber optic fiber Bragg grating (FBG) sensing technology has been emerging as a strong alternative that could provide solutions for advanced in situ sensing within electric machine geometries. Its inherent features of electromagnetic interference (EMI) immunity, small size, power passivity, flexibility, and ability to multiplex sensing provide opportunities to overcome many of the existing limitations with sensing used in electric machine CMs [10–12]. While FBG sensors are inherently responsive to mechanical and thermal excitation, they can be adapted to measure other physical phenomena of interest in electromagnetic rotary devices, such as through the integration of magnetostrictive material for magnetic flux measurement [13–15]. Despite the wider adoption of FBG sensing in electric machinery still being stifled by its relatively high cost, much effort has been reported in recent years on exploring effective ways to implement FBGs in various electric machine types to enable advanced multi-physical in situ sensing. This is extended to other associated power equipment where the unique FBG sensing features invariably present attractive opportunities for the in-service observation of high-fidelity device measurements.

This paper presents a review of the current state of the art and advances in FBG sensing research for electric machinery by providing a summary of the current knowledge of FBG sensors' usage and application requirements for effective CM. This is a rapidly developing area of great interest to users, designers, and operators of electric machinery alike, with a potential to overcome the many barriers in how these devices are operated and utilized by allowing higher fidelity and targeted insights into relevant multi-physical in-service measurands hitherto unavailable through the application of conventional sensing. The aim is to provide an up-to-date summary of the many FBG sensing techniques that are increasingly proposed for electric machinery and deliver an evaluation of the progress, trends, and outlook in this topic that can inform and stimulate further developments. In addition, modern machines are invariably driven by power electronic converters where machine operation and integrity and that of the converter are inherently linked. FBG technology has a strong potential to facilitate improved in situ sensing for power electronic devices as well as other machine-associated power equipment (e.g., that used in high voltage machinery applications); hence, recent advances in applying the FBG sensing to monitor these are also reviewed for the sake of completeness.

2. Operating Principles of FBG Sensors

FBG sensors are increasingly commercially available and are, today, one of the most popular sensors from the fiber optic sensing family, having found use in a variety of industrial and research applications. A conventional FBG sensor is made up of a specially fabricated small and flexible segment imprinted into the core of a single-mode optical fiber, as illustrated in Figure 1.

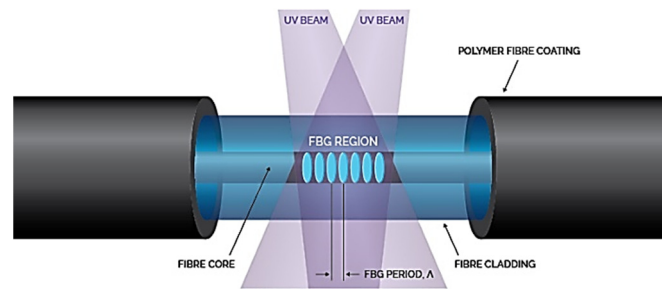


Figure 1. Structure of an FBG sensor [16].

Figure 1 shows a typical FBG sensor structure, with a single-mode optical fiber containing a cylindrical core (glass, from 4 to 9 μm in diameter) which is surrounded by a cladding layer (glass, 125 μm in diameter). The purpose of the cladding layer is to confine light propagation within the glass core and limit optical losses. Furthermore, the top coating layer, which is generally made of acrylate or polyimide, is applied to strengthen the fiber. The sensing part of the structure is denoted as the FBG sensing head and comprises an equidistant sequence of gratings, which are UV (ultraviolet) laser-induced modulations in the glass core refractive index during FBG fabrication. The length of the FBG sensor (FBG head length) is defined by the number of gratings and the distance between them (grating period Λ) and is typically in a range from 1 to 20 mm [17]. Multiple sensing heads can be manufactured on the same fiber in a variety of available structures to provide a multiplexed sensor array on a single fiber strand.

When the fiber is illuminated by broadband light, the gratings reflect a specific light spectrum (i.e., the Bragg wavelength, λ_B), which varies with the thermal and mechanical conditions that the sensing head is exposed to. The light wavelength that is reflected meets the Bragg condition as set by the grating structure, while the rest of the light spectrum is transmitted through the FBG head. The operation principle of an FBG sensor is illustrated in Figure 2, where λ_B is the calculated peak mid-point of the reflected wavelength. Assuming other relevant application conditions are satisfied, monitoring the reflected spectrum can enable the FBG head to principally be utilized as a thermal and/or mechanical sensing device with the advantages of EMI immunity, a small size, and flexibility.

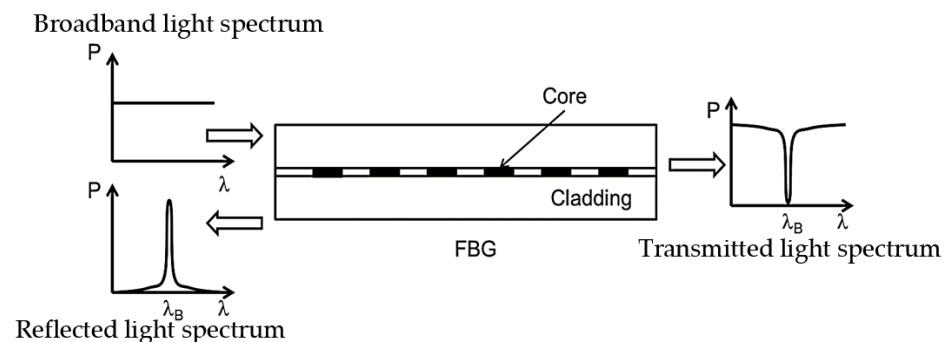


Figure 2. Operating principles of FBG.

In a sensing application, an FBG head reflects a specific wavelength of light from a distinct fiber location exposed to physical excitation, such as temperature, strain, etc. The measurement process involves the observation and measurement of the reflected wavelength using a specialized optoelectronic interrogator device. Once acquired, the reflected wavelength is converted to a set physical measurand, based on a pre-calibrated wavelength for the physical excitation relationship [15,18]. In principle, an interrogator is responsible for illuminating the fiber, and subsequently, for successfully receiving and monitoring the reflected Bragg wavelength(s). Depending on the nature of a particular sensing application, the interrogator needs to capture any rapid changes in the wavelength,

and therefore, different techniques are available for the effective tracking of the relative changes in λ_B . Overall, the general characteristics that are required from the integrator used in FBG sensing are high resolution, high accuracy, usually within the range of pico meters, multiplexing ability, and acceptable cost. In addition, the calibration process of the wavelength shift to the physical measurement value is imperative for enabling FBG sensing applications [11,19]. This involves the exposure of the sensor to a controlled range of the physical measurand to be observed, and the characterization of the reflected wavelength to the physical measurand value relationship. Where possible, calibration is performed on free FBG fibers, however, some applications can require in situ sensor calibration, which can be challenging due to the sensor being embedded within a device and the use of any required sensor-to-device structure bonding media.

A typical reflected wavelength spectrum of an FBG sensor is illustrated in Figure 3.

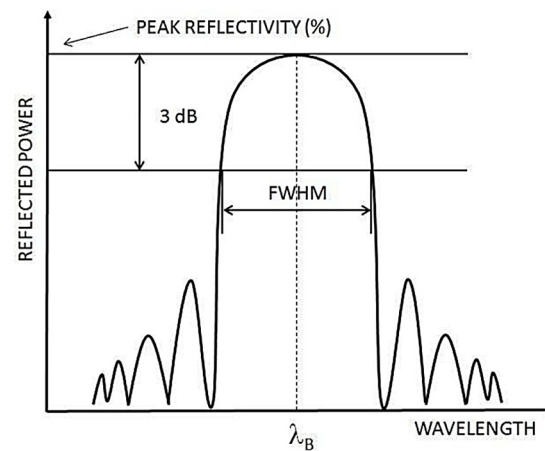


Figure 3. A reflected wavelength spectrum of a typical FBG sensor [20].

The bandwidth of the FBG sensor reflection is defined as its full width at half maximum (FWHM) and is the reflected spectra width at 50% or -3 dB from the peak reflection point. The bandwidth of an FBG sensor is dependent on a number of FBG structure parameters, notably the grating number and spacing [20]. The peak wavelength of the reflected narrowband is the Bragg reflection wavelength, λ_B , which is dependent on the effective refractive index of the optical fiber (n_{eff}) and the Bragg grating period (Λ , i.e., the spacing between successive gratings) and can be calculated as [17]:

$$\lambda_B = 2 n_{eff} \Lambda \quad (1)$$

Any change in the observed measurand, such as strain and temperature, results in a corresponding change in n_{eff} and Λ , and therefore, results in a consequent variation in λ_B , which is calculated as [17]:

$$\frac{\Delta\lambda_B}{\lambda_B} = \left\{ 2 \left[\Lambda \frac{\partial n_{eff}}{\partial \varepsilon} + n_{eff} \frac{\partial \Lambda}{\partial \varepsilon} \right] \Delta\varepsilon \right\} + \left\{ 2 \left[\Lambda \frac{\partial n_{eff}}{\partial T} + n_{eff} \frac{\partial \Lambda}{\partial T} \right] \Delta T \right\} \quad (2)$$

In (2): $\Delta\lambda_B$ is the relative change in the reflected Bragg wavelength, ε is the strain, and T is temperature. The first term in brackets in (2) is related to the Bragg wavelength shift caused by the strain-induced elastic-optic effect, whereas thermo-optic and thermal expansion caused by the Bragg wavelength variation are represented in the second term in (2). For ease of interpretation, Equation (2) can be presented in the literature be in its condensed form as:

$$\frac{\Delta\lambda_B}{\lambda_B} = \{k_\varepsilon \Delta\varepsilon\} + \{k_T \Delta T\} \quad (3)$$

where k_ε is the total strain and k_T is the total temperature sensitivity factor of the FBG sensor.

3. FBG Sensing Application in Electric Machines

FBG monitoring for in situ sensing applications in electrical machines has received increased research attention due to the number of advantages it can inherently provide for installation and monitoring within machine geometries, including [21–24]:

- Immunity to EMI,
- Lower signal-to-noise ratio,
- Electrical passivity, including at the measuring point,
- Flexibility, compactness, and small size,
- The potential for long in-service life,
- Resistance to harsh environments (e.g., extreme temperatures, moisture, corrosion, etc.)
- A multiplexing ability enabling distributed sensing schemes, and,
- A multi-physical sensing capability.

The key operational and health parameters of electric machines, such as vibration, rotor speed, torque, the temperature in stator windings and on the rotor, as well as the air-gap flux density and others, have been shown to have the potential to measure in-service using FBG sensing systems [4]. The operating principles and installation requirements of these applications are reviewed in this section.

3.1. Thermal Sensing

Temperature is one of the key parameters that affect the operational characteristics and performance of an electric machine. Generally, the principal source of thermal stress in machines is their wound components. The thermal stress resulting from high winding temperatures can cause the degradation of the insulation and ensure damage to the circuit components, leading to a reduction in the machine's lifetime and eventual failure. Approximately 40% of failures in induction machines are reported to be caused by winding insulation breakdown and the resulting thermal stress [21]. Furthermore, as the main contributor to the overall heat produced within an electric machine, the windings can affect the thermal status of all other components. For example, the resultant excess heat can also negatively affect the performance of permanent magnet elements, which is present, or in severe cases, lead to their demagnetization. An increased winding temperature from the nominal level, even if moderate and not extreme, generally leads to an increase in the losses and increase in lifetime consumption, and thus a reduction in machine performance, and is hence undesirable. Effective temperature monitoring is, therefore, key to ensuring motor reliability and optimal performance. This predominantly relates to the stator and rotor wound components; however, it is also pertinent to the rotor bearings, as these are machine-critical components that are degraded by the excess friction caused by heat. The key aim of thermal monitoring is to achieve the early detection of local overheating and, consequently, a reduction in the maintenance cost and optimization of performance. This can be attained through the effective monitoring of temperature in hotspot locations of interest in machine wound components and bearings [25].

The conventional temperature monitoring approach in electric machines generally employs embedded temperature sensors, such as thermocouples (TCs) or resistance thermal detectors (RTDs), to measure the local temperature of the monitored parts [26]. However, the utilization of these sensors, especially for critical machine applications, can have considerable limitations due to the safety risks posed by the electrically conductive nature of the sensor material and the sensor installation complexity; further constraints arise from the physical dimensions of these sensors, which can prevent or significantly complicate the effective access to key thermal measurement locations of interest (e.g., windings slots) [27]. The conventional TC and RTD-based thermal sensing are additionally challenged where the monitoring of machine rotary components is concerned, suffering from installation and wiring complexity and challenges around data transmission between the rotating rotor and a stationary external sensing platform [28,29]. The application of FBG sensing to monitor the electric machine temperature, with its multitude of inherent advantages for sensing

in confined and harsh environments, has been gaining attention as a viable alternative to traditional temperature sensing systems.

The principle of measuring temperature using FBG sensors is based on the identification of $\Delta\lambda_B$ caused by temperature variation. Heat has several effects on the optical fiber and its gratings, including changes in the grating period, as well as the thermo-optic effect related to the dependency of n_{eff} on temperature. The reflected wavelength shift due to temperature change is calculated using the fiber thermal characteristics and ignoring the mechanical excitation, which can be obtained as [30]:

$$\Delta\lambda_B = \lambda_B(\alpha + \xi)\Delta T \quad (4)$$

where α is the fiber thermal expansion coefficient ($\approx 0.55 \times 10^{-6}/\text{K}$) and ξ is the fiber thermo-optic coefficient ($\approx 6.67 \times 10^{-6}/\text{K}$) [31]. The thermal sensitivity for a standard bare FBG with the Bragg wavelength of 1550 nm operating at ambient temperature is $\approx 10 - 14 \text{ pm}/^\circ\text{C}$ [17]. The thermal measurement is, however, complicated by the inherent thermo-mechanical cross-sensitivity of FBG fibers, as defined in Equation (2). In essence, for an unpackaged bare FBG head, it can be expected that the sensor will respond to both thermal and mechanical excitation. Thus, if an unpackaged sensor is placed in a location where it is exposed to thermal and mechanical excitation, it will respond to both.

To ensure an exclusively thermal measuring ability, an FBG sensor needs to be insulated from mechanical excitation. This is commonly achieved by packaging the sensor in an external geometry made of a material suitable for a given sensing application: the purpose of packaging is to contain the sensing head in a location protected from mechanical excitation (stress and strain). Further to this, the packaging should ideally possess suitable thermal properties to allow for the adequate observation of the thermal measurement change and also be electrically passive/nonconductive [11,18]. Different packaging layouts and materials have been researched in the literature and are aimed at facilitating the stator temperature monitoring; small diameter and wall thickness thermoplastic polymer (Polyether ether ketone (PEEK)) tubes [11,32] were used to package FBG sensors and embed them in low voltage random wound windings, and tubes made of steel and copper [33] were used to package the thermal sensors located in the stator slot openings or stator winding radiators, respectively. In the study, [11] applied the temperature measurements provided by the winding in situ FBG sensor to estimate the remaining lifetime of the motor winding in operation. PEEK packaging, in particular, makes it possible to wind the packaged thermal sensor(s) into the desired location within the coil geometry and to monitor thermal hotspots internal to the winding structure in a minimally invasive fashion and safely, as PEEK is an electrically passive material with adequate mechanical properties. In [31], it was shown that the application of PEEK-packaged FBG thermal sensors in PMSM machine windings could allow the detection of winding faults by monitoring the localized thermal changes produced by the fault. The integration of FBG sensors within the microplastic winding insulation material in large power generators was also performed and showed good immunity to mechanical excitation industrial electronics. In general, the application of the electrically passive PEEK packaged FBG sensing for stator winding embedded thermal monitoring is the optimal application for this technique, which is currently reported in the literature for this application.

Thermal measurements for rotor temperature monitoring have been established [4,34,35] by the application of fiber optic rotary joints (FORJs). This allows an optical contact to be established between the FBG sensors installed on the moving rotor and a stationary interrogator so that thermal readings from rotor locations can be taken. An array of thermal sensing points can then be established by employing a single fiber carrying multiple multiplexed FBG heads to observe the in-service conditions on PM and induction machine rotors or, where necessary or convenient, to use multiple separate fibers. Due to the limited space on the rotor in smaller machine geometries and the general challenges imposed by rotor movement in all-electric machinery, the applied FBG sensors have typically been bonded to the desired rotor locations using epoxy resin or cyanoacrylate glue; this can result in

the inclusion of mechanical excitation related artifacts in the observed measurements [36,37]. While this is functional and able to facilitate continuous in-service thermal monitoring, this method is reasonably costly and challenging for practical implementation in typical power conversion applications of electric machines due to the relatively high cost of the FORJ device and the requirements for its in-line installation on the machine shaft. These limitations would, however, be much less severe in larger scale (cost) electric machinery such as, e.g., large power generators. The application of a FORJ is the only known method to extract FBG measurements from the rotary component of electrical machinery.

Thermal sensing applications in bearings have also been prototyped and shown as feasible [33,38–40]. FBG sensors have been integrated within the bearing structure in machined surface grooves using adhesives, implemented in externally fixed polymer structures, and used as standalone sensor devices for large power generator bearing and coolant temperature measurements. Multiplexing was applied to establish distributed thermal sensing arrays in the bearing geometry and monitor changes in-service, with or without the presence of defects, achieving good results. The sensor application embedded within the bearing structure imposes more invasive requirements for installation of this technology in comparison with the methods based on the application of an externally fixed and removable/reusable polymer structure containing FBG sensors. While the sensitivity of these two methods would need to be directly compared to ascertain which is optimal and would likely favor the direct application method, it can be shown that the external coupling method can allow for the recognition of defects while retaining the advantage of being removable/reusable and more straightforward for application.

Various local and distributed thermal monitoring schemes for electric machines have been examined in the literature and are summarized in terms of their machine application type, sensor location, and measurand features in Table 1 for clarity and completeness.

Table 1. Examples of FBG-based temperature monitoring applications on electric machines.

Reference	Type of Electric Machine	Sensor Location	Monitored Temperature
[7]	A 3.7 kW induction motor	Above the slot wedges in the slot openings	Stator temperature distribution under healthy operation
[41]	A 3.7 kW induction motor	Above the slot wedges in the slot openings	Mechanical and core losses related to temperature rise in the stator
[4]	A 2 kW permanent-magnet motor	Axially across the stator slot openings	Temperature distribution of stator windings
[25]	A 200 MVA air-cooled power generator	On the stator winding copper bars	Stator copper bars temperature distribution under normal operation
[42]	A 1000 MW power generator	On the stator conductor top bar surface	Quasi-distributed thermal measurement of the stator windings' inner temperature
[43]	A large, air-cooled power generator	On the stator winding copper bars	FBG sensing system operating in harsh environment
[44]	A 175 MW synchronous generator	Into small grooves between the stator surface insulation and the rotor poles	Stator surface temperature under transient start-up and normal operating conditions of a hydroelectric plant
[4]	A 2 kW permanent magnet motor	On the moving rotor structure	The temperature of rotor magnets
[34]	A 75 MVA hydro generator	An FBG-distributed sensing system in the rotor	Field windings
[37]	A 74.5 MVA hydro generator	On the rotor winding surface	Rotor field windings based on investigating the effects of thermo-mechanical stresses in an FBG sensor assembly
[45]	A 5.5 kW permanent magnet synchronous machine	On multiple thermal sensing points distributed within the stator end-winding section	Stator end-winding under different healthy and faulty operating conditions
[46]	A 180 MW hydro generator	In the generator bearing	The generator bearing temperature increases due to shaft misalignment
[33]	A 42.5 MW hydro generator	An FBGs array with five FBG heads in the stator	The stator generator temperature during start-up and in operation

Table 1. Cont.

Reference	Type of Electric Machine	Sensor Location	Monitored Temperature
[36]	A 0.55 kW induction motor	Two FBG heads were attached to the cage rotor: one on the rotor bar surface and the other on the end-ring	Using a fiber optic rotating joint (FORJ) rotor temperature rise level with load increase was monitored
[34,35]	A 310 MVA generator	An FBG was used at the rotor's axis	The generator field winding temperature
[38]	A 0.55 kW induction motor	On the outer race bearing	Temperature rises on the healthy and faulty bearings at three different load conditions (no load, half load, and full load)

3.2. Mechanical Sensing

Monitoring mechanical parameters, such as the frame vibration or strain and/or vibration in different machine locations, is a recognized method of electric machine condition monitoring and is often stipulated by appropriate certification standards in various machine applications [1,2,8,47,48]. The conventional approach to mechanical sensing utilizes accelerometer sensors mounted externally on the machine frame and, where available, in larger machines distributed within the machine geometry in other positions of interest (e.g., large generator end windings). The FBG's inherent ability to measure strain and the possibility to utilize this feature to design FBG-based accelerometer sensors [49,50] combined with other attractive FBG features presents a number of opportunities for the development of advanced localized and/or distributed strain and acceleration monitoring schemes.

In addition, operating speed monitoring in electric machines is essential for their effective usage and control. This is usually measured using encoder and resolver sensors; however, these can be compromised in challenging environments [27]. There is a general interest, therefore, in employing the inherent ability of FBG sensing for conceiving speed sensing schemes in rotating machines which could yield gains in increased robustness, smaller sensor packages, etc. [3].

The observation of shaft torque is also of considerable interest in the utilization and testing of electric machinery [9,51]. This is usually achieved by the installation of a bulky in-line transducer on the test machine shaft and has considerable limitations in practical usage. Methods that could facilitate less demanding torque sensing are, therefore, of considerable interest, presenting another area of mechanical sensing in electric machinery where the FBG sensing application could be attractive.

3.2.1. Strain Sensing

FBG strain sensors have been applied for the conditional monitoring of applications in electric machinery. FBG sensors were bonded to the machine frame in [52] to observe the in-service surface strain. It was shown that distinct signatures in the observed surface strain signal could be identified in the presence of stator electrical faults that could allow a diagnosis to be made of a stator winding fault presence. FBG strain sensors were also installed between the stator teeth (see Figure 4 for illustration) within an induction machine geometry and were bonded by cyanoacrylate glue to observe the operating strain in the presence of a rotor broken bar fault and rotor dynamic eccentricity [53,54]. It was found that the observed strain spectral content contained clearly defined magnitudes at the fault frequency caused by the specific fault-created stator deformation and the consequent distortion in electromagnetic forces; this allows the localized strain measurement to be used for the recognition of fault presence. Furthermore, FBG strain sensing was applied in machine ball bearings for monitoring the in-service surface strain, demonstrating the presence of distinct fault frequencies with rotating elements and raceway faults [38,40]. It was shown that all the aforementioned fault spectral signatures in the strain signal were speed-dependent and could, in principle, be trended for fault monitoring and diagnosis in dynamic operating conditions.

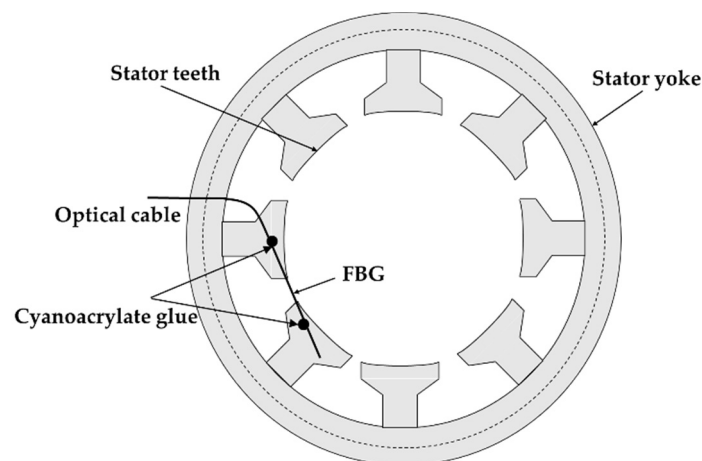


Figure 4. FBG strain sensor placement on the stator teeth [53].

In summary, available research has demonstrated that in situ strain sensing within electric machine geometries is feasible with FBG sensors and that the signatures of electromagnetic and mechanical forces arising with distinct fault modes can be identified and trended through this measurement. This shows that the application of in situ FBG strains envisaged for the observation of relative strain is adequate for general CM purposes; however, further research is needed on the in situ monitoring of absolute in-service strain values, which could provide valuable insights into the actual level of strain associated with fault inception and propagation, as well as insights into in-service strain levels in healthy machinery.

3.2.2. Torque Sensing

FBG sensors have been applied in schemes aimed at shaft torque measurements [3–5,55]. The approach relied on utilizing two FBG strain sensors mounted on the rotor in the axial plane at +45 and –45 degrees with respect to the axis of rotation: this allowed the differential wavelength approach to be used to extract dynamic measurements of the shaft torque, including primarily the torque DC component, and limited, first order rotational speed frequency components. The method still requires more extensive testing and analysis of the measurands to warrant wider application but is, however, still unique in addressing the torque sensing application of FBG technology in electric machines.

3.2.3. Vibration Sensing

The monitoring of vibration in electric machines is vital to facilitate the effective detection of mechanical faults (e.g., bearing faults) but can also enable the recognition of electrical faults and asymmetry [9,24,51,56]. Various FBG vibration sensor schemes have been explored in the literature and can generally be classified into two groups based on the sensing principle employed and the installation method: the contact sensors and the non-contact sensors [26]. The study in [57] presents a non-contact FBG vibration sensor which is based on the conversion of the observed distance between the sensor and the machine shaft into the magnetic force. The vibration of the rotating shaft is hence obtained through the observation of the FBG sensor wavelength shift. FBG accelerometers are classed as contact FBG vibration sensors and measure the Bragg wavelength shift of the FBG when related to the acceleration of a vibrating assembly [58]. The operation principle of the FBG accelerometers is based on transferring the observed acceleration to the FBG strain variation. This typically requires the integration of an FBG strain-sensing fiber into an external structure that is able to perform the acceleration-to-strain conversion. A cantilever FBG accelerometer design for the machine vibration measurement was examined in [58] and is illustrated in Figure 5.

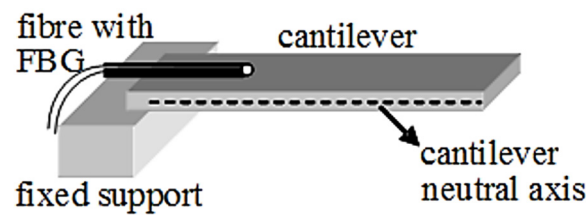


Figure 5. A 3D view of cantilever-based FBG accelerometer [58].

The cantilever converts any acceleration imposed on it into a strain [59,60], which is then sensed by the cantilever-embedded FBG sensor. The sensor was designed from composite materials to ensure that it was nonconductive and thus suitable for application in electric machines. Furthermore, two polymers were used in its construction with different elasticity characteristics to enhance sensitivity. The sensor was tested in standalone shaker experiments and demonstrated to have good performance potential.

An FBG accelerometer using a single mode fiber containing two identical FBGs, which are placed generally 5 mm to 20 mm apart from each other and embedded in a polyamide diving board structure, can act as an acceleration-to-strain converter, as illustrated in Figure 6, which was used for large generator end winding narrowband monitoring and was shown to reliably function [24]. An adaptation of this design was explored to allow wider band vibration monitoring for general electric machinery monitoring purposes showing promise but also requiring further refinement for more effective use [61].

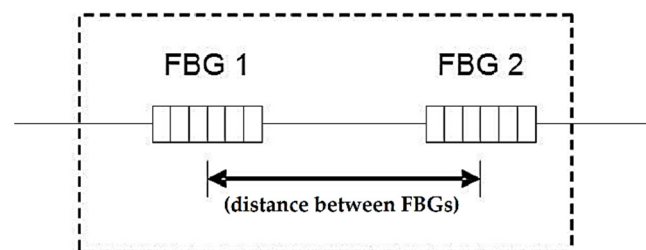


Figure 6. Systematic diagram FBG vibration sensor head [62].

An in-line fiber etalon (ILFE) sensor has a unique feature of the seismic mass effect with two different ranges of operation, including the ability to work as an accelerometer below the resonance frequency and working as a vibrometer for higher frequencies (the sensor output is proportional to displacement) and has been used to monitor the vibration of induction motors working at a steady-state under voltage unbalance [60]. The vibration measurement of an induction motor running at a no-load condition using a biaxial optical fiber accelerometer, which comprises four FBGs to measure the biaxial vibration, is presented in [56]. The biaxial vibration sensor measures the acceleration via the difference between the Bragg wavelength shift of two gratings per direction. This study shows that the biaxial optical accelerometer exhibits good reliability in monitoring machine vibrations when compared with a commercial capacitive accelerometer. An alternative approach is taken in [56], where FBG sensors were bonded to the adjacent stator core teeth to observe core deformation and, thus, infer information on machine vibration and detect machine static and dynamic rotor eccentricity faults [56].

In summary, multiple different approaches have been taken to FBG-enabled acceleration sensing, with most manifesting relative limitations in the sensing bandwidth. Further research is needed to extend this to more effectively cater to the frequencies of interest in the CM of electric machinery, especially, those in higher speed machinery.

3.2.4. Rotational Speed Sensing

Refs. [4,5,63] examine an FBG sensing-based scheme that allows the simultaneous observation of speed and position in an electrical motor. The fundamental idea is to monitor

the stator core's vibratory response/displacement using FBGs as a function of the air-gap flux modulation and then analyze this measurand and infer the rotating speed and field position information. In this application, a fiber with circumferentially mounted FBG sensors between the stator teeth was used to measure position and speed by measuring the strain due to the mechanical displacement of the stator teeth. The method was reported to exhibit promising results.

3.3. Magnetic Field Sensing Application

FBG sensing methods have been developed for magnetic field sensing applications in electrical machines. The FBGs can be used for magnetic field measurement by combining the FBG strain sensing capability with magnetostrictive material properties [64–66]. The FBG strain sensing utilized in this application was conceptually distinct from the strain sensing described in Section 3.2.1, in which the strain was generated by bonding on the surface of electrical machines (e.g., machine frame [52]). In contrast, the strain in the FBG magnetic field sensing application was excited by the magnetostrictive material as a result of the exposure to a magnetic field. When a magnetic field is applied to a magnetostrictive material, the material will change its shape and become strained: if this strain can be monitored in situ by an FBG sensor integrated with the magnetostrictive material structure, then the strain measurand can be converted to a flux-to-yield flux sensing ability.

Terfenol-D is an iron and rare earth metal alloy that has been associated with the largest known levels of magnetostriction at room temperature [67]. This material can be applied as a compact piece with the FBGs directly bonded to it (see Figure 7a) [12,15,68,69] or as a composite formed by a mix of Terfenol-D powder and a suitable adhesive, with FBGs submerged within its structure, as shown in Figure 7b [13,14,70].

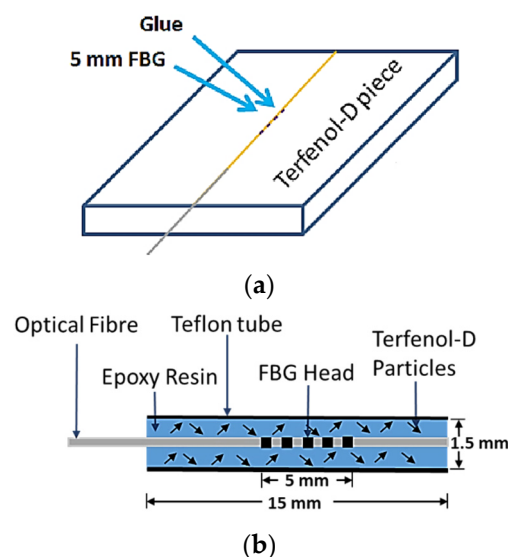


Figure 7. The FBGs sensor designs for magnetic field monitoring applications. (a) With a solid piece Terfenol-D [12] (b) With magnetostrictive composite material [13].

The FBG magnetic field sensor has been used and developed for electric machine applications, including the condition monitoring of induction motors [70], permanent magnet synchronous machines (PMSMs) [13–15,71], and large hydro generators [68,72]. In [70], a hole was made in the stator core, and an FBG magnetic field sensor was installed in it for the observation of air gap flux and, thus, the detection of broken rotor bars in an induction motor (IM). The sensor was based on FBG and a magnetostrictive composite made of Terfenol-D material submerged with the epoxy resin matrix, as illustrated in Figure 8. A single FBG Terfenol-D sensor was embedded on a retrofitted slot wedge installed in a stator slot mouth of a PMSM to monitor the PM rotor demagnetization faults [14,15,71]. Figure 9 shows the sensor application for monitoring the air-gap flux

density to examine the demagnetized surface PM rotor conditions. The air-gap flux density of a radial magnetic bearing was measured by using FBGs in [69], where two sensors were placed in opposite magnetic fields at the stator to complement the temperature differences. In [72], FBG technology and magnetostrictive material (Terfenol-D) were presented at integration which offered a noninvasive sensor for online magnetic field monitoring in large hydro generators to detect rotor winding defects caused by inter-turn short circuits. The application of FBG flux sensing for stray flux monitoring in induction machines and, hence, stator winding fault detection was explored in [73]. The sensor used was a nickel-coated FBG, where nickel-coating geometric deformation with a magnetic field change was used as a medium of flux to strain the conversion. The application of a Terfenol-D composite-based FBG flux sensor for the external monitoring of induction motor stray flux and winding fault signature monitoring was studied in [74] and reported fault-specific Bragg wavelength shift changes; however, the findings and depth of analysis were limited by the low scan rate of the optical analyzer used in this research.

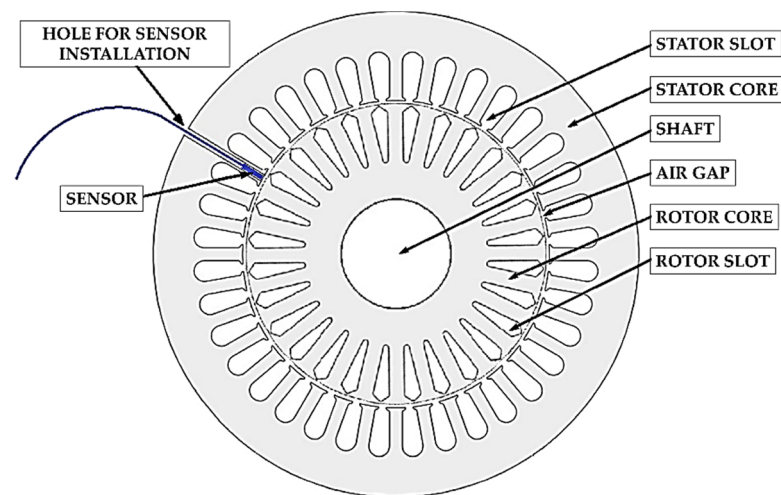


Figure 8. IM broken rotor bars monitoring [70].

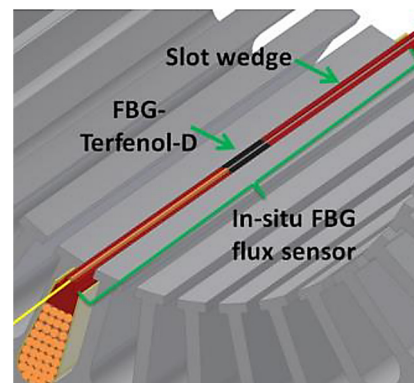


Figure 9. In situ FBG flux sensor to monitor air-gap flux density in PMSM [15].

Table 2 shows examples of FBGs applications in electric machine magnetic field condition monitoring. Most promising results have been reported through the usage of Terfenol D, whether in solid or powder form. Further research on the temperature cross-sensitivity of these would also be needed to demonstrate the viability of a long-term flux measurement in service.

Table 2. FBGs for EM magnetic field monitoring applications.

Reference	Type of Electric Machine	Sensor Location	Monitored Magnetic Field
[70]	A 0.75 kW induction motor	In a hole made in the stator core	Air-gap field to monitor broken rotor bars
[15]	A 1.1 kW PMSM	On the slot wedge	Air-gap field at different PM rotor demagnetization levels
[72]	A 200 MVA hydro generator	On the ventilation ducts of the stator core	Air-gap field to detect inter-turn short circuits of the rotor windings
[14]	A single-coil 1.1 kW PMSM	On the slot wedge	Air-gap field at different PM rotor demagnetization levels
[73]	A 1.1 kW three-phase induction motor	Above the silicon steel sheet	Stray-flux monitoring during three different fault scenarios on the end-winding

3.4. High Voltage Application

High voltage (HV) equipment is an integral part of any electrical power system, and in addition to traditional use in large-scale energy production, HV electrical machinery, in particular, is gaining increasing interest in a range of applications, e.g., aerospace and marine electric transport systems. High voltage assets also include equipment, such as cables, overhead line conductors, transformers, switch gear, and other major substation assets. All of this electrical infrastructure, much of it past its original service life, will experience increased stresses (electrical, thermal, and mechanical) with the increase in peak demand and the variation of load profiles due to low carbon technologies and harsher environmental conditions. Understanding the aging mechanisms and monitoring conditions based on the temperature, vibration, and electric field provides vital asset health information and minimizes unplanned downtime (and possible blackouts on the network) due to failures.

FBG sensors provide a unique opportunity to measure all the above mechanisms, with the added benefit of being able to be installed within a high-voltage environment. The passive nature of the sensors can be exploited by installing them within high-voltage assets, such as transformers, to monitor temperature and hot spot detection [75–77]. The failure of such equipment is mostly brought on by insulation damage (which can be caused due to the combination of thermal, mechanical, and electrical aging), which is typically preceded by an increasing level of partial discharge (PD) due to insulation degradation. PD is caused by the breakdown of insulation due to voids, defects, and high electric fields. PD is, therefore, widely monitored in HV equipment using an array of different methods, including electrical, acoustic, chemical, and optical methods. The study in [78] focuses on a PD detector based on an FBG sensor and a mandrel, which, consequently, significantly increases the sensitivity of the sensor. The FBG has a wide bandwidth response, and depending on the diameter of the mandrel, the received signal will be amplified at certain frequencies. In [79], a multiplexed PD sensing method for power transformers is presented. The work also investigates the sensitivity of phase-shifted FBG sensors for partial discharge-generated ultrasonic emissions.

Marignetti et al. [80] proposed and illustrated a method for using FBG sensors to measure the electric field in the HV generator end winding region. A conventional FBG was used in the construction of the sensor and was operated based on the inherent electrostrictive properties of silica with no need for bulky electrostrictive material head packaging. The sensor performance was validated in tests on a 1–20 kV range parallel-plate electric field generator. Studies [81,82] introduced an intensity-modulated FBG photodetection sensor intended for HV equipment application. The high-frequency acoustic wave that was created as a result of the occurrence of PD could be detected by the proposed sensor and has been validated in tests in comparison with the standard contact type PD measurement. In the [83,84] study, the application of an FBG cavity sensor for PD monitoring in HV generator windings was performed. The sensor diving board structure is mounted onto a ceramic board to enhance the sensitivity to higher PD representative frequencies;

the testing of the sensor was limited but showed performance potential in a simulating sparking scenario. The fundamental principles of PD and electric field FBG sensing in high voltage electric machinery are reasonably well understood; however, despite the sizeable market for these applications, the FBG sensing solutions have not been standardized, nor are they commercially mature at a scale that would support a large-scale use. Further research is needed to improve the sensitivity of these methods and standardize the optimal sensor architectures for these applications.

3.5. Multiphysical Sensing Application

The exploitation of the FBG sensors' inherent multi-physical sensing ability has been gaining interest in devising sensing devices able to observe multiple measurements simultaneously. The inherent thermo-mechanical sensitivity of FBGs could, in principle, be exploited for multi-physical sensing applications involving the monitoring of temperature and mechanical strains (or magnetic flux, electric field, etc., proportional to it) using a single FBG head. This sensing method has recently emerged as a potentially useful option for the multi-physical monitoring of the condition of electric machines, largely driven by the initial study reported in [38,39] using FBGs for healthy and faulty bearing condition monitoring in an induction machine. An FBG sensor was used to monitor the in-situ thermal and mechanical conditions in a bearing structure by installing the sensor on the outer race of the motor end-drive bearing (see Figure 10). It was reported that, due to the inherent thermo-mechanical sensitivity of the FBG sensors and the different sensitivity to these measurands, combined with an inherent difference in the nature of thermal and mechanical excitation in the electric machine bearings, it was possible to obtain simultaneously thermal and mechanical measurements from a single sensing head fitted on the bearing. One measurement here is absolute while the other is relative; however, it was demonstrated that this could be sufficient for condition monitoring purposes in a case study examining in-service rolling element fault detection. The study [36] investigated the viability of deriving simultaneously localized in-service information on the induction motor rotor temperature and strain from a single FBG sensing head bonded to the rotor surface. A shaft in-line and installed fiber optic rotary joint (FORJ) was used to interface the rotor installed with FBGs and an external stationary interrogator. Figure 11 shows the adapted commercial FORJ that was used for this application. Study [40] further explored the FBG inherent multi-physical sensing principles to establish thermal and mechanical condition monitoring in an induction machine bearing for an inner raceway fault. In this study, an FBG array sensor with three FBG heads was encapsulated in the carbon-fiber-reinforced polymer for increased mechanical protection and ease of installation, demonstrating good performance in tests on an operating machine. A simultaneous relative flux and absolute temperature sensing scheme through the application of a single nickel-coated FBG sensing head in the induction machine end windings was explored in [73] and reported an effective performance in in-service tests.

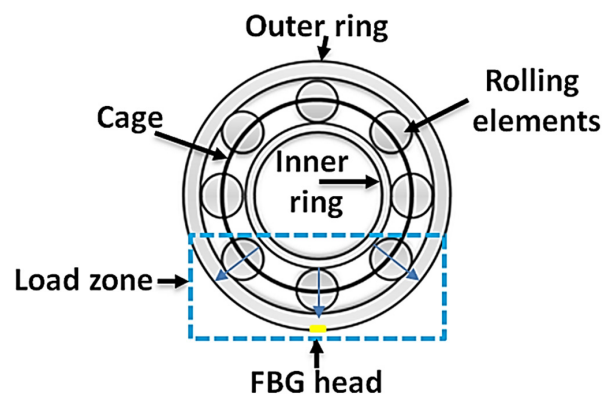


Figure 10. The FBG head position for multi-physical bearing monitoring [38,39].

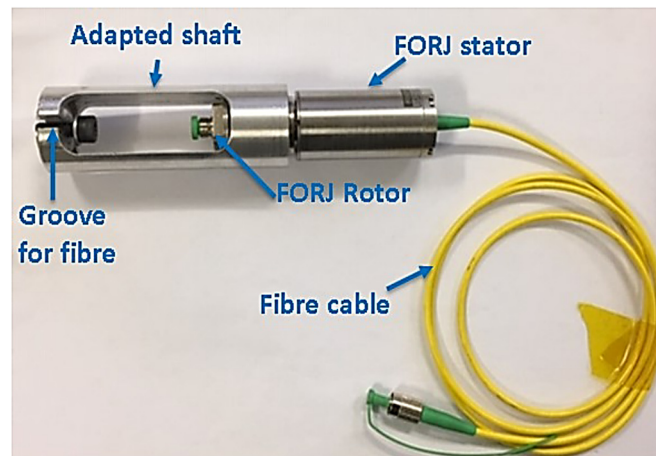


Figure 11. The commercial fiber optic rotating joint (FORJ) [36].

While the simultaneous capture of multiple multi-physical measurements from a single sensing head is of interest, the advanced distributed and multi-physical measuring ability can also be achieved by installing multiple dedicated FBG sensors at specific positions within an electrical machine. Study [3–5] used 48 FBGs installed within a PMSM: 24 FBGs placed along the stator windings for in-situ temperature profiling; 12 FBGs were circumferentially attached to the stator core to detect the vibration, rotor speed, position, and the air gap field frequency and rotation direction; and the final 12 FBGs were placed in one fiber on the rotor surface and shaft for multi-parameter rotor sensing (thermal and torque), as illustrated in Figure 12. For the rotor sensing application, a FORJ was used to enable sensor interrogation while the rotor was spinning.

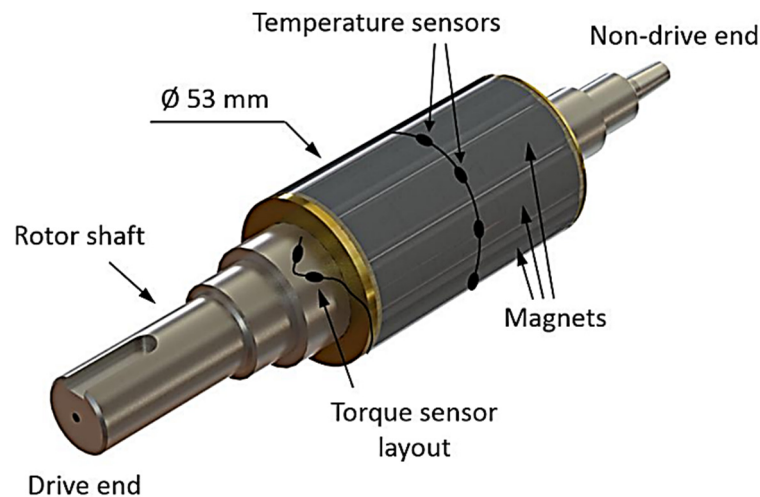


Figure 12. Multi-parameter sensing in the PMSM rotor [5].

Table 3 summarizes the leading works in the area of FBG application for multi-physical monitoring within electrical machinery. Multi-physical sensing applications research is still in its relative infancy; however, it has shown potential for facilitating powerful, single-sensor measurement methods, with an imposed limitation for one measurand to be relative. Further research is needed to explore this principle in further locations and with the combination of physical measurements of interest.

Table 3. FBGs for multi-physical parameter monitoring applications.

Reference	Type of Electric Machine	Sensor Location	Monitored Parameters
[38,39]	A 0.55 kW induction motor	On the end-drive bearing outer race	Thermal and mechanical strain parameters at different load and faulty conditions
[36]	A 0.55 kW induction motor	On the rotor bar and the end-ring surfaces	Thermal and mechanical operating conditions
[40]	A 15 HP induction motor	On the ball bearing cover	Thermal and mechanical strain for an inner race bearing fault condition.
[3–5,85]	A 2 kW PM motor	In the stator winding and stator teeth, on the PM rotor, and on the rotor shaft	Thermal profiling, mechanical vibration, and torque.
[73]	A 1.1 kW three-phase induction motor	Above the silicon steel sheet	Temperature measurement and magnetic sensing during three fault conditions on the end-winding

3.6. Power Electronics Device Sensing Application

Modern electrical machine applications are invariably in a power electronic inverter-driven format, where the operation of the machine is directly linked to and dependent on that of the inverter. The monitoring of power inverter operating parameters is, thus, of increasing importance, with the thermal monitoring of power electronic switches being of paramount interest in this respect [86–88]. The vital thermal measurement of interest is commonly the switch junction temperature, where conventional sensing devices, such as TCs and RTDs, are challenged and impractical/impossible to use. FBG size and EMI immunity can offer considerable advantages in this application and provide the ability to monitor further physical measurements of interest [19,89–97]. This is a growing research area with limited work currently available where studies on the direct on-chip FBG sensing applications on standard insulated gate bipolar transistor (IGBT) devices have largely revolved around exploring the possibility of acquiring accurate point temperatures.

Study [8] explores the application of an IGBT module base embedded packaged FBG array for the distributed thermal monitoring of the module IGBT chips and diodes. While reportedly flexible and functional, the scheme measures the baseplate locations' thermal conditions and requires the application of thermal models to infer the thermal conditions on actual module chips. Study [1] utilized a low thermal tolerance mineral oil bond to interface the FBG sensor to the IGBT chip surface for direct junction temperature monitoring and reported limited results at a low current temperature only. The findings were incorporated into the construction of a thermal model that was used to replicate the heat produced by the device when it was conducting and switching. The model demonstrated a good agreement between the measured and simulated findings.

A scheme utilizing an array sensor to measure the temperature distribution in the upper silicon layer of the IGBT module was presented in [2]; the reported validation tests are, however, performed only at the close of an ambient temperature and the observed temperatures are not in the on-chip hotspot locations of interest. Study [89] explores an enhanced sensitivity FBG thermal sensor application for the IGBT temperature measurement in a photovoltaic array inverter. An FBG sensor was bonded at each side of the sensing head to a steel plate to utilize its higher thermal expansion coefficient to increase the Bragg wavelength shift and, thus, the thermal sensing sensitivity. The plate-bonded FBG sensor was installed between the IGBT and its heatsink and seemed to provide improved sensitivity and linearity. Study [3] examined the FBG sensor application for distributed thermal monitoring in a 5-MW generator exciter bridge. FBGs were encapsulated in steel tubes and glued on thyristor heatsinks for temperature measurements. While not providing the on-device thermal hotspot monitoring of key interest, the method was tested in-service and was shown to provide a good measurement performance.

The application of FBG sensors for direct IGBT on-chip thermal sensing for loss estimation was studied in [4]. Limited information was provided on the sensor-to-chip interfacing, and limited test results involving a few switch cycles only were presented, while no research was undertaken on in-service sensing features and performance. Study [92] examined the direct IGBT temperature sensing using a thermal paste bonded FBG and a free FBG positioned on the chip surface, as illustrated in Figure 13. Experiments and simulations using finite elements were used to compare the performance of two different sensor interface configurations. The scheme was tested on a commercial IGBT module and was shown to provide good results in a dynamic operating scenario within the chip's nominal operating range.

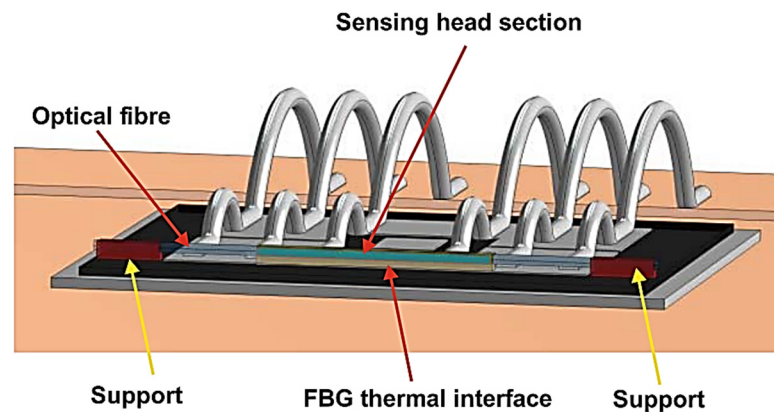


Figure 13. The FBGs installation on the commercial IGBT module [92].

The effect of the FBG head length influence on the quality of the observed localized temperature measurement on the IGBT surface was studied in [95] and indicated the importance of considering the surface sensing location, the chip surface inherent thermal gradient, and the head length for a reliable measurement to be achieved. Longer sensing heads were found to generate errors in the measurement due to the Bragg wavelength modulation caused by the uneven thermal excitation imposed on the sensor and arising from the chip surface's uneven thermal distribution.

Refs. [90,91] examined the FBG sensor application in a press pack IGBT power module for in-service distributed temperature monitoring. Different sensor layouts, including tube packaged and metal platelet bonded sensors were evaluated, and a good potential of FBG sensors which bonded to the chip surface to enable temperature monitoring, was reported for the emerging press pack chip geometry. Several possible FBG sensor integration strategies are outlined and assessed regarding their functionality in the context of a practical converter operation. Study [90] explores the FBG sensor application for contact pressure monitoring in press pack modules. The FBG measurement of the contact pressure is facilitated by converting the pressure to strain (through modifying the module's spring stack structure), which is then measured by the press pack module integrated FBGs. While some thermo-compensation issues were identified, it was shown that the proposed scheme was promising for contact pressure monitoring.

4. Outlook and Conclusions

This paper has presented a systematic overview of FBG sensing applications in electric machines and associated power equipment. The variety of the presented sensing methods indicates clearly that FBG sensing can play a significant role in facilitating embedded, in-situ sensing in electric machinery that cannot be matched by conventional sensing. This includes the provision for the observation of various multi-physical measurands, such as temperature, strain, velocity, vibration, flux, etc., in device-embedded locations of interest which are not accessible by other sensing means. This sensing ability has the potential to unlock considerable diagnostic advantages, as well as those which more accurately characterize the features and limits of a given machine or drive design. As such, in-situ

FBG sensing can present a highly useful means of improving the reliability and performance of electric machinery. Its acceptance and more common application in this context, however, is largely dominated by its application cost, which currently remains higher than that of the standard, more limited CM systems. Furthermore, while the state-of-the-art reports many diverse methods for achieving the FBG-based sensing of various measurands within operating machinery, further research is needed to try and standardize the best practice in the distinct sensing areas from both the functional, but also the cost perspective. This is equally pertinent to, e.g., standard thermal monitoring in stationary wound components, as well as advanced in-situ multi-physical sensing.

While FBG sensors are comparable in cost to conventional alternatives and, in some cases, cheaper (e.g., flux sensing), the interrogator box remains the key bottleneck in the wider adoption of these sensors in electrical machines and drive sectors. With the possible prospects of a wider market application, such as, e.g., dedicated thermal sensing systems for electric vehicle traction motors, this cost could be driven down to see FBG sensors become a more mainstream sensing option while providing an advanced sensing ability. The current state, however, is such that FBG schemes are considerably more acceptable as research and development support monitoring techniques for device prototype performance characterization or model validation, improvement, and calibration. This excludes high-value assets (e.g., power generators and similar) where the cost of the application of FBG systems and the diagnostic and monitoring advantages they can deliver is far outweighed by the application and downtime value, and thus, FBG usage can become more acceptable.

Author Contributions: Conceptualization, A.A.S., N.S., A.M., V.P., and S.D.; methodology, S.D.; investigation, A.A.S., N.S., S.D.; writing—original draft preparation, A.A.S., N.S., V.P., and S.D.; writing—review and editing, A.A.S., N.S., A.M., V.P., and S.D.; visualization, A.A.S., N.S., and S.D. All authors have read and agreed to the published version of the manuscript.

Funding: The Government of Indonesia Endowment Fund: S-1013/LPDP4/2019.

Institutional Review Board Statement: Not applicable.

Informed Consent Statement: Not applicable.

Data Availability Statement: Not applicable.

Acknowledgments: This study was partially supported by the Indonesia Endowment Fund for Education (LPDP) Ministry of Finance, and the Republic of Indonesia in Jakarta.

Conflicts of Interest: The authors declare no conflict of interest.

Abbreviations

Symbol/Abbreviation	Description
FBG	Fiber Bragg Grating
EMI	Electromagnetic interference
CM	Condition monitoring
UV	Ultraviolet
FWHM	Full width at half maximum
λ_B	Bragg wavelength
n_{eff}	Effective refractive index of the optical fiber
Λ	The Bragg grating period
$\Delta\lambda_B$	The relative change in reflected Bragg wavelength
ε	Strain
k_ε	The total strain sensitivity factor
k_T	The total temperature sensitivity factor
TC	Thermocouple
RTD	Resistance thermal detector
α	the fiber thermal expansion coefficient
ξ	The fiber thermo-optic coefficient

T	Temperature
PEEK	Polyether ether ketone
FORJ	Fiber optic rotating joint
ILFE	In-line fiber etalon
PMSM	Permanent magnet synchronous machine
IM	Induction motor
HV	High voltage
PD	Partial discharge
IGBT	Insulated gate bipolar transistor

References

1. Tavner, P.; Ran, R.; Penman, J.; Sedding, H. *Condition Monitoring of Rotating Electrical Machines*; The Institution of Engineering and Technology: London, UK, 2008; p. 306. [\[CrossRef\]](#)
2. Toliyat, H.A.; Nandi, S.; Choi, S.; Meshgin-kelk, H. *Electric Machines: Modeling, Condition Monitoring, and Fault Diagnosis*; CRC Press: Boca Raton, FL, USA, 2013. [\[CrossRef\]](#)
3. Hind, D.; Gerada, C.; Galea, M.; Bartolo, J.B.; Fabian, M.; Sun, T.; Grattan, K.T.V. Use of Optical Fibres for Multi-parameter Monitoring in Electrical AC Machines. In Proceedings of the 2017 IEEE 11th International Symposium on Diagnostics for Electrical Machines, Power Electronics and Drives (SDEMPED), Tinos, Greece, 29 August–1 September 2017. [\[CrossRef\]](#)
4. Fabian, M.; Hind, D.M.; Gerada, C.; Sun, T.; Grattan, K.T.V. Comprehensive Monitoring of Electrical Machine Parameters Using an Integrated Fiber Bragg Grating-Based Sensor System. *J. Light. Technol.* **2018**, *36*, 1046–1051. [\[CrossRef\]](#)
5. Fabian, M.; Hind, D.; Gerada, C.; Sun, T.; Grattan, K.T.V. Multi-Parameter Monitoring of Electrical Machines Using Integrated Fibre Bragg Gratings. In Proceedings of the 2017 25th Optical Fiber Sensors Conference (OFS), Jeju, Republic of Korea, 24–28 April 2017. [\[CrossRef\]](#)
6. Mellor, P.; Roberts, D.; Turner, D. Lumped Parameter Thermal Model for Electrical Machines of TEFC design. In Proceedings of the IEEE Proceedings B—Electric Power Applications, September 1991. [\[CrossRef\]](#)
7. Sousa, K.D.M.; Hafner, A.A.; Crespim, M.; Somenzi, J.; De Oliveira, V.; Kalinowski, H.J.; Da Silva, J.C.C. Fiber Bragg Grating Sensing Applications in Temperature Monitoring of Three-Phase Induction Motors. In Proceedings of the 2011 SBMO/IEEE MTT-S International Microwave and Optoelectronics Conference (IMOC 2011), Natal, Brazil, 29 October–1 November 2011. [\[CrossRef\]](#)
8. Tavner, P.J. Review of Condition Monitoring of Rotating Electrical Machines. *IET Electr. Power Appl.* **2008**, *2*, 215–247. [\[CrossRef\]](#)
9. Sarma, N.; Tuohy, P.; Djurović, S. Condition Monitoring of Rotating Electrical Machines. In *Reference Module in Materials Science and Materials Engineering*; Elsevier: Amsterdam, The Netherlands, 2022. [\[CrossRef\]](#)
10. Sousa, K.M.; Bazzo, J.P.; Mezzadri, F.; Bortolotti, F.; Martelli, C.; Silva, J.C.C.; Probst, W.K. Optical Fiber Bragg Grating Sensors Applied on Energy Conversion Systems. In Proceedings of the 2013 SBMO/IEEE MTT-S International Microwave & Optoelectronics Conference (IMOC), Rio de Janeiro, Brazil, 4–7 August 2013. [\[CrossRef\]](#)
11. Mohammed, A.; Djurovic, S. FBG Thermal Sensing Features for Hot Spot Monitoring in Random Wound Electric Machine Coils. *IEEE Sens. J.* **2017**, *17*, 3058–3067. [\[CrossRef\]](#)
12. Melecio, J.I.; Mohammed, A.; Djurović, S. Characterisation of FBG based Magnetic Field Sensor Response Sensitivity to Excitation Orientation for Rotating Electric Machine Applications. In Proceedings of the 2019 8th Mediterranean Conference on Embedded Computing (Meco), Budva, Montenegro, 10–14 June 2019. [\[CrossRef\]](#)
13. Suryandi, A.A.; Damian, I.E.; Djurović, S. FBG Magnetostrictive Composite Flux Sensor Response Characterisation for Surface Permanent Magnet Rotor Flux Monitoring. In Proceedings of the 2021 10th Mediterranean Conference on Embedded Computing (MECO), Budva, Montenegro, 7–10 June 2021; pp. 1–6. [\[CrossRef\]](#)
14. Suryandi, A.A.; Djurovic, S. FBG Magnetostrictive Composite Flux Sensor for Monitoring Rotor Permanent Magnet Flux. In Proceedings of the 2022 11th Mediterranean Conference on Embedded Computing (MECO), 7–10 June 2022; pp. 1–6. [\[CrossRef\]](#)
15. Mohammed, A.; Melecio, J.I.; Djurovic, S. Electrical Machine Permanent Magnets Health Monitoring and Diagnosis Using an Air-gap Magnetic Sensor. *IEEE Sens. J.* **2020**, *20*, 5251–5259. [\[CrossRef\]](#)
16. Fibres, S. FBG Sensing System. Available online: <https://www.smartfibres.com/technology> (accessed on 14 October 2022).
17. Rao, Y.-J. In-fibre Bragg grating sensors. *Meas. Sci. Technol.* **1997**, *8*, 355–375. [\[CrossRef\]](#)
18. Mohammed, A.; Djurović, S. A study of distributed embedded thermal monitoring in electric coils based on FBG sensor multiplexing. *Microprocess. Microsyst.* **2018**, *62*, 102–109. [\[CrossRef\]](#)
19. Mohammed, A.; Hu, B.; Hu, Z.; Djurović, S.; Ran, L.; Barnes, M.; Mawby, P.A. Distributed Thermal Monitoring of Wind Turbine Power Electronic Modules Using FBG Sensing Technology. *IEEE Sens. J.* **2020**, *20*, 9886–9894. [\[CrossRef\]](#)
20. Werneck, M.M.; Allil, R.C.S.B.; Ribeiro, B.A.; Nazaré, F.V.B. *A Guide to Fiber Bragg Grating Sensors: Current Trends in Short- and Long-Period Fiber Gratings*; InTech: Rijeka, Croatia, 2013; pp. 1–24. [\[CrossRef\]](#)
21. Mohammed, A.; Djurovic, S.; Smith, A.; Tshiloz, K. FBG Sensing for Hot Spot Thermal Monitoring in Electric Machinery Random Wound Components. In Proceedings of the 2016 XXII International Conference on Electrical Machines (ICEM), Lausanne, Switzerland, 4–7 September 2016. [\[CrossRef\]](#)
22. Fajkus, M.; Nedoma, J.; Martinek, R.; Fridrich, M.; Bednar, E.; Zabka, S.; Zmij, P. Pressure Membrane FBG Sensor Realized by 3D Technology. *Sensors* **2021**, *21*, 5158. [\[CrossRef\]](#)

23. Wang, Y.; Mohammed, A.; Sarma, N.; Djurović, S. Double Fed Induction Generator Shaft Misalignment Monitoring by FBG Frame Strain Sensing. *IEEE Sens. J.* **2020**, *20*, 8541–8551. [[CrossRef](#)]
24. Kung, P.; Wang, L.; Comanici, M.I. Stator end Winding Vibration and Temperature Rise Monitoring. In Proceedings of the 2011 Electrical Insulation Conference (EIC), Annapolis, MD, USA, 5–8 June 2011; pp. 10–14. [[CrossRef](#)]
25. Theune, N.M.; Muller, M.; Hertsch, H.; Kaiser, J.; Willsch, M.; Krammer, P.; Bosselmann, T. Investigation of Stator Coil and Lead Temperatures on High Voltage Inside Large Power Generators via Use of Fiber Bragg Gratings. In Proceedings of the SENSORS, 2002 IEEE, Orladno, FL, USA, 12–14 June 2002; Volume 1602, pp. 1603–1607. [[CrossRef](#)]
26. Shang, K.; Zhang, Y.; Galea, M.; Brusica, V.; Korposh, S. Fibre optic sensors for the monitoring of rotating electric machines: A review. *Opt. Quantum Electron.* **2020**, *53*, 1–28. [[CrossRef](#)]
27. Shang, K.; Galea, M.; Brusica, V.; Korposh, S.; Zhang, Y. Polyimide-Coated Fibre Bragg Grating (FBG) Sensors for Thermal Mapping of Electric Machine Windings. In Proceedings of the 2020 22nd International Conference on Transparent Optical Networks (ICTON), Bari, Italy, 19–23 July 2020; pp. 1–4. [[CrossRef](#)]
28. Popov, N.Z.; Vukosavic, S.N. Estimator of the Rotor Temperature of Induction Machine Based on Terminal Voltages and Currents. *IEEE Trans. Energy Convers.* **2017**, *32*, 155–163. [[CrossRef](#)]
29. Ying, W.; Hongwei, G. Induction-motor stator and rotor winding temperature estimation using signal injection method. *IEEE Trans. Ind. Appl.* **2006**, *42*, 1038–1044. [[CrossRef](#)]
30. Kersey, A.D.; Davis, M.A.; Patrick, H.J.; LeBlanc, M.; Koo, K.P.; Askins, C.G.; Putnam, M.A.; Friebele, E.J. Fiber grating sensors. *J. Light. Technol.* **1997**, *15*, 1442–1463. [[CrossRef](#)]
31. Mohammed, A.; Melecio, J.I.; Djurovic, S. Open-Circuit Fault Detection in Stranded PMSM Windings Using Embedded FBG Thermal Sensors. *IEEE Sens. J.* **2019**, *19*, 3358–3367. [[CrossRef](#)]
32. Tshiloz, K.; Smith, A.C.; Mohammed, A.; Djurovic, S.; Feehally, T. Real-Time Insulation Lifetime Monitoring for Motor Windings. In Proceedings of the 2016 XXII International Conference on Electrical Machines (ICEM), Lausanne, Switzerland, 4–7 September 2016. [[CrossRef](#)]
33. Werneck, M.M.; Allil, R.C.D.S.B.; Ribeiro, B.A. Calibration and Operation of a Fiber Bragg Grating Temperature Sensing System in a Grid-Connected Hydrogenerator. *IET Sci. Meas. Technol.* **2013**, *7*, 59–68. [[CrossRef](#)]
34. Hudon, C.; Guddemi, C.; Gingras, S.; Leite, R.C.; Mydlarski, L. Rotor Temperature Monitoring Using Fiber Bragg Gratings. In Proceedings of the Electrical Insulation Conference (EIC), Montreal, QC, Canada, 19–22 June 2016. [[CrossRef](#)]
35. Hudon, C.; Lévesque, M.; Essalihi, M.; Millet, C. Investigation of rotor hotspot temperature using Fiber Bragg Gratings. In Proceedings of the IEEE Electrical Insulation Conference (EIC), Baltimore, MD, USA, 19–22 June 2017. [[CrossRef](#)]
36. Mohammed, A.; Djurović, S. Rotor Condition Monitoring Using Fibre Optic Sensing Technology. In Proceedings of the 10th International Conference on Power Electronics, Machines and Drives (PEMD 2020), Online Conference, 15–17 December 2020; pp. 92–97. [[CrossRef](#)]
37. Leite, R.; Dmitriev, V.; Hudon, C.; Gingras, S.; Guddemi, C.; Piccard, J.; Mydlarsky, L. Analysis of Thermo-Mechanical Stress in Fiber Bragg Grating Used for HydroGenerator Rotor Temperature Monitoring. *J. Microw. Optoelectron. Electromagn. Appl.* **2017**, *16*, 445–459. [[CrossRef](#)]
38. Mohammed, A.; Djurović, S. Electric Machine Bearing Health Monitoring and Ball Fault Detection by Simultaneous Thermo-Mechanical Fibre Optic Sensing. *IEEE Trans. Energy Convers.* **2021**, *36*, 71–80. [[CrossRef](#)]
39. Mohammed, A.; Djurovic, S. In-Situ Thermal and Mechanical Fibre Optic Sensing for In-Service Electric Machinery Bearing Condition Monitoring. In Proceedings of the 2019 IEEE International Electric Machines & Drives Conference (IEMDC), San Diego, CA, USA, 12–15 May 2019. [[CrossRef](#)]
40. Pelegrin, J.d.; Dreyer, U.J.; Sousa, K.M.; Silva, J.C.C.d. Smart Carbon-Fiber Reinforced Polymer Optical Fiber Bragg Grating for Monitoring Fault Detection in Bearing. *IEEE Sens. J.* **2022**, *22*, 12921–12929. [[CrossRef](#)]
41. Sousa, K.M.; Hafner, A.A.; Kalinowski, H.J.; da Silva, J.C.C. Determination of Temperature Dynamics and Mechanical and Stator Losses Relationships in a Three-Phase Induction Motor Using Fiber Bragg Grating Sensors. *IEEE Sens. J.* **2012**, *12*, 8. [[CrossRef](#)]
42. Wang, P.; Liu, J.; Song, F.; Zhao, H. Quasi-Distributed Temperature Measurement for Stator Bars in Large Generator via Use of Fiber Bragg Gratings. In Proceedings of the Proceedings of 2011 6th International Forum on Strategic Technology, Heilongjiang, Harbin, China, 22–24 August 2011. [[CrossRef](#)]
43. Weidner, J. Direct Measurement of Copper Conductor Temperature at Generator Windings with Fibre Bragg Grating (FBG) Sensors. *SC A1 Rotating Mach. Contrib. PS1 Q* **2012**, *1*.
44. Cicero, M.; da Erlon Vagner, S.; Kleiton de Moraes, S.; Felipe, M.; Jonas, S.; Marcos, C.; Hypolito José, K.; Jean Carlos Cordoza da, S. Temperature Sensing in a 175MW Power Generator. In Proceedings of the OFS2012 22nd International Conference on Optical Fiber Sensors, Beijing, China, 14 October 2012; p. 84212F. [[CrossRef](#)]
45. Mohammed, A.; Djurovic, S. FBG Thermal Sensing Ring Scheme for Stator Winding Condition Monitoring in PMSMs. *IEEE Trans. Transp. Electrification* **2019**, *5*, 1370–1382. [[CrossRef](#)]
46. Uilian José, D.; da Erlon Vagner, S.; André Biffe Di, R.; Felipe, M.; Hypolito José, K.; Valmir de, O.; Cicero, M.; Jean Carlos Cardozo da, S. Fiber Optic Temperature Sensing in Heat Exchangers and Bearings for Hydro Generators. *J. Microw. Optoelectron. Electromagn. Appl.* **2015**, *14*, SI-35–SI-44.
47. Benbouzid, M.; Berghout, T.; Sarma, N.; Djurović, S.; Wu, Y.; Ma, X. Intelligent Condition Monitoring of Wind Power Systems: State of the Art Review. *Energies* **2021**, *14*, 5967. [[CrossRef](#)]

48. DNVGL. Certification of condition monitoring. *Serv. Specif.* **2016**, DNVGL-SE-0439. Available online: <https://standards.globalspec.com/std/10022130/dnvgl-se-0439> (accessed on 10 October 2022).
49. Berkoff, T.A.; Kersey, A.D. Experimental demonstration of a fiber Bragg grating accelerometer. *IEEE Photonics Technol. Lett.* **1996**, *8*, 1677–1679. [[CrossRef](#)]
50. Stefani, A.; Andresen, S.; Yuan, W.; Herholdt-Rasmussen, N.; Bang, O. High Sensitivity Polymer Optical Fiber-Bragg-Grating-Based Accelerometer. *IEEE Photonics Technol. Lett.* **2012**, *24*, 763–765. [[CrossRef](#)]
51. Tavner, P.; Ran, L.; Crabtree, C. *Condition Monitoring of Rotating Electrical Machines*, 3rd ed.; IET: London, UK, 2020. [[CrossRef](#)]
52. Mohammed, A.; Sarma, N.; Djurović, S. Fibre Optic Monitoring of Induction Machine Frame Strain as a Diagnostic Tool. In Proceedings of the 2017 IEEE International Electric Machines and Drives Conference (IEMDC), Miami, FL, USA, 21–24 May 2017. [[CrossRef](#)]
53. Sousa, K.M.; Dreyer, U.J.; Martelli, C.; da Silva, J.C.C. Dynamic Eccentricity Induced in Induction Motor Detected by Optical Fiber Bragg Grating Strain Sensors. *IEEE Sens. J.* **2016**, *16*, 4786–4792. [[CrossRef](#)]
54. Sousa, K.D.M.; Dreyer, U.J.; Martelli, C.; da Silva, J.C.C. Vibration Measurement of Induction Motor under Dynamic Eccentricity Using Optical Fiber Bragg Grating Sensors. In Proceedings of the 2015 SBMO/IEEE MTT-S International Microwave and Optoelectronics Conference (IMOC), Porto de Galinhas, Brazil, 3–6 November 2016. [[CrossRef](#)]
55. Wang, Y.; Liang, L.; Yuan, Y.; Xu, G.; Liu, F. A Two Fiber Bragg Gratings Sensing System to Monitor the Torque of Rotating Shaft. *Sensors* **2016**, *16*, 138. [[CrossRef](#)]
56. Linessio, R.P.; Sousa, K.D.M.; Silva, J.C.C.d.; Antunes, P.F.D.C. Analysis of Vibrations in Electrical Machines with an Optical Fiber Accelerometer. In Proceedings of the 2015 SBMO/IEEE MTT-S International Microwave and Optoelectronics Conference (IMOC), Porto de Galinhas, Brazil, 3–6 November 2015; pp. 1–5. [[CrossRef](#)]
57. Li, T.; Tan, Y.; Zhou, Z.; Cai, L.; Liu, S.; He, Z.; Zheng, K. Study on the non-contact FBG vibration sensor and its application. *Photonic Sens.* **2015**, *5*, 128–136. [[CrossRef](#)]
58. Basumallick, N.; Bhattacharya, S.; Dey, T.K.; Biswas, P.; Bandyopadhyay, S. Wideband Fiber Bragg Grating Accelerometer Suitable for Health Monitoring of Electrical Machines. *IEEE Sens. J.* **2020**, *20*, 14865–14872. [[CrossRef](#)]
59. Antunes, P.F.d.C.; Lima, H.F.T.; Alberto, N.J.; Rodrigues, H.; Pinto, P.M.F.; Pinto, J.d.L.; Nogueira, R.N.; Varum, H.; Costa, A.G.; Andre, P.S.d.B. Optical Fiber Accelerometer System for Structural Dynamic Monitoring. *IEEE Sens. J.* **2009**, *9*, 1347–1354. [[CrossRef](#)]
60. Corres, J.M.; Bravo, J.; Arregui, F.J.; Matias, I.R. Unbalance and harmonics detection in induction motors using an optical fiber sensor. *IEEE Sens. J.* **2006**, *6*, 605–612. [[CrossRef](#)]
61. Wei, B.; Wang, X.; Wang, Y.; Zhong, H. Online Monitoring System for Motor Vibration Using Fiber Bragg Grating Sensing Technology. In Proceedings of the 2011 International Conference on Electrical Machines and Systems, Beijing, China, 20–23 August 2011; pp. 1–3. [[CrossRef](#)]
62. Vilchis-Rodriguez, D.; Djurovic, S.; Kung, P.; Comanici, M.I.; Smith, A.C. Investigation of Induction Generator Wide Band Vibration Monitoring Using Fibre Bragg Grating Accelerometers. In Proceedings of the 2014 International Conference on Electrical Machines (ICEM), Berlin, Germany, 2–5 September 2014. [[CrossRef](#)]
63. Fabian, M.; Bartolo, J.B.; Ams, M.; Gerada, C.; Sun, T.; Grattan, K.T.V. Vibration Measurement of Electrical Machines Using Integrated fibre Bragg Gratings. In Proceedings of the 24th International Conference on Optical Fibre Sensors, Curitiba, Brazil, 28 September–2 October 2015; p. 963417. [[CrossRef](#)]
64. Schukara, V.; Köppea, E.; Hofmanna, D.; Westphala, A.; Sahrea, M.; Gongga, X.; Bartholmaia, M.; Becka, U. Magnetic Field Detection with an Advanced FBG-Based Sensor Device. In Proceedings of the 30th Eurosensors Conference, EUROSENSORS 2016, Berlin, Germany, 4–7 September 2016. [[CrossRef](#)]
65. Li, M.; Zhou, J.; Xiang, Z.; Lv, F. Giant Magnetostrictive Magnetic Fields Sensor Based on Dual Fiber Bragg Gratings. In Proceedings of the IEEE Networking, Sensing and Control, Tucson, AZ, USA, 19–22 March 2005. [[CrossRef](#)]
66. Hristoforou, E.; Ktena, A. Magnetostriction and magnetostrictive materials for sensing applications. *J. Magn. Magn. Mater.* **2007**, *316*, 372–378. [[CrossRef](#)]
67. Dapino, M.J.; Deng, Z.; Calkins, F.T.; Flatau, A.B. Magnetostrictive Devices. *Wiley Encycl. Electr. Electron. Eng.* **2016**, 1–35. [[CrossRef](#)]
68. Fracarolli, J.; Floridaia, C.; Rosolem, J.B.; Leonardi, A.A.; Dini, D.C.; Dilli, P.I.G.; Da Silva, E.V.; Dos Santos, M.C.; Fruett, F. High-speed FBG Interrogation System Insensitive to Fiber Link Attenuation for Magnetic Field Sensing. In Proceedings of the 24th International Conference on Optical Fibre Sensors, Curitiba, Brazil, 28 September–2 October 2016. [[CrossRef](#)]
69. Ding, G.; Zhang, S.; Cao, H.; Gao, B.; Zhang, B. Flux Density Measurement of Radial Magnetic Bearing with A Rotating Rotor Based on Fiber Bragg Grating-Giant Magnetostrictive Material Sensors. *Appl. Opt.* **2017**, *56*, 4975–4981. [[CrossRef](#)] [[PubMed](#)]
70. Bieler, G.; Werneck, M.M. A magnetostrictive-fiber Bragg grating sensor for induction motor health monitoring. *Measurement* **2018**, *122*, 117–127. [[CrossRef](#)]
71. Suryandi, A.A.; Tuohy, P.; Djurovic, S. Finite Element Analysis Study of FBG Magnetostrictive Composite Flux Sensor Geometry for Electric Motor Air-gap Flux Monitoring. In Proceedings of the 2022 11th Mediterranean Conference on Embedded Computing (MECO), Budva, Montenegro, 7–10 June 2022; pp. 1–6. [[CrossRef](#)]
72. Fracarolli, J.P.V.; Rosolem, J.B.; Tomiyama, E.K.; Floridaia, C.; Penze, R.S.; Peres, R.; Dini, D.C.; Hortencio, C.A.; Dilli, P.I.G.; Silva, E.V.d.; et al. Development and field trial of a FBG-based magnetic sensor for large hydrogenerators. *Fiber Opt. Sens. Appl.* **2016**, *9852*, 154–162. [[CrossRef](#)]

73. Wu, Y.H.; Liu, M.Y.; Song, H.; Li, C.; Yang, X.L. A Temperature and Magnetic Field-Based Approach for Stator Inter-Turn Fault Detection. *IEEE Sens. J.* **2022**, *22*, 17799–17807. [[CrossRef](#)]
74. Cao, W.; Alalibo, B.P.; Ji, B.; Chen, X.; Hu, C. Optical FBG-T Based Fault Detection Technique for EV Induction Machines. *J. Phys. Conf. Ser.* **2022**, *2195*, 012045. [[CrossRef](#)]
75. Ribeiro, A.B.L.; Eira, N.F.; Sousa, J.M.; Guerreiro, P.T.; Salcedo, J.R. Multipoint Fiber-Optic Hot-Spot Sensing Network Integrated into High Power Transformer for Continuous Monitoring. *IEEE Sens. J.* **2008**, *8*, 1264–1267. [[CrossRef](#)]
76. Onn, B.I.; Arasu, P.T.; Al-Qazwini, Y.; Abas, A.F.; Tamchek, N.; Noor, A.S.M. Fiber Bragg Grating Sensor for Detecting Ageing Transformer Oil. In Proceedings of the 2012 IEEE 3rd International Conference on Photonics, Pulau Pinang, Malaysia, 1–3 October 2012; pp. 110–113. [[CrossRef](#)]
77. Kuhn, G.G.; Sousa, K.M.; Martelli, C.; Bavastri, C.A.; Silva, J.C.C.d. Embedded FBG Sensors in Carbon Fiber for Vibration and Temperature Measurement in Power Transformer Iron Core. *IEEE Sens. J.* **2020**, *20*, 13403–13410. [[CrossRef](#)]
78. Ghorat, M.; Gharehpetian, G.B.; Latifi, H.; Hejazi, M.A.; Layeghi, A. Partial discharge acoustic emission detector using mandrel-connected fiber Bragg grating sensor. *Opt. Eng.* **2018**, *57*, 074107. [[CrossRef](#)]
79. Ma, G.M.; Zhou, H.Y.; Shi, C.; Li, Y.B.; Zhang, Q.; Li, C.R.; Zheng, Q. Distributed Partial Discharge Detection in a Power Transformer Based on Phase-Shifted FBG. *IEEE Sens. J.* **2018**, *18*, 2788–2795. [[CrossRef](#)]
80. Marignetti, F.; Santis, E.d.; Avino, S.; Tomassi, G.; Giorgini, A.; Malara, P.; Natale, P.D.; Gagliardi, G. Fiber Bragg Grating Sensor for Electric Field Measurement in the End Windings of High-Voltage Electric Machines. *IEEE Trans. Ind. Electron.* **2016**, *63*, 2796–2802. [[CrossRef](#)]
81. Sarkar, B.; Koley, C.; Roy, N.K.; Kumbhakar, P. Condition monitoring of high voltage transformers using Fiber Bragg Grating Sensor. *Measurement* **2015**, *74*, 255–267. [[CrossRef](#)]
82. Sarkar, B.; Mishra, D.K.; Koley, C.; Roy, N.K.; Biswas, P. Intensity-Modulated Fiber Bragg Grating Sensor for Detection of Partial Discharges Inside High-Voltage Apparatus. *IEEE Sens. J.* **2016**, *16*, 7950–7957. [[CrossRef](#)]
83. Kung, P.; Wang, L.; Comanici, M.I.; Chen, L.R. Detection and Location of PD Activities Using an Array of Fiber Laser Sensors. In Proceedings of the IEEE International Symposium on Electrical Insulation, San Juan, PR, USA, 10–13 June 2012. [[CrossRef](#)]
84. Kung, P.; Wang, L.; Pan, S.; Comanici, M.I. Adapting the FBG cavity Sensor Structure to Monitor and Diagnose PD and Vibration Sparking in Large Generator. In Proceedings of the Electrical Insulation Conference, Ottawa, ON, Canada, 2–5 June 2013. [[CrossRef](#)]
85. Sun, T.; Fabian, M.; Chen, Y.; Vidakovic, M.; Javdani, S.; Grattan, K.T.V.; Carlton, J.; Gerada, C.; Brun, L. Optical Fibre Sensing: A Solution for Industry. In Proceedings of the 2017 25th Optical Fiber Sensors Conference (OFS), Jeju, Republic of Korea, 24–28 April 2017; pp. 1–4. [[CrossRef](#)]
86. Riera-Guasp, M.; Antonino-Daviu, J.A.; Capolino, G. Advances in Electrical Machine, Power Electronic, and Drive Condition Monitoring and Fault Detection: State of the Art. *IEEE Trans. Ind. Electron.* **2015**, *62*, 1746–1759. [[CrossRef](#)]
87. Manohar, S.S.; Sahoo, A.; Subramaniam, A.; Panda, S.K. Condition Monitoring of Power Electronic Converters in Power Plants—A Review. In Proceedings of the 2017 20th International Conference on Electrical Machines and Systems (ICEMS), Sidney, Australia, 11–14 August 2017; pp. 1–5. [[CrossRef](#)]
88. Song, J.; Zhao, J.; Dong, F.; Zhao, J.; Qian, Z.; Zhang, Q. A Novel Regression Modeling Method for PMSLM Structural Design Optimization Using a Distance-Weighted KNN Algorithm. *IEEE Trans. Ind. Appl.* **2018**, *54*, 4198–4206. [[CrossRef](#)]
89. Tamchek, N.; Michael, A.P.; Sandoghchi, S.R.; Hassan, M.R.; Dambul, K.D.; Selvaraj, J.; Rahim, N.A.; Adikan, F.R.M. Design, characterization and implementation of a fiber Bragg grating temperature sensor for application in solar power electronic inverters. *Appl. Sol. Energy* **2011**, *47*, 184–188. [[CrossRef](#)]
90. Ren, H.; Liu, L.; Djurovic, S.; Ran, L.; Liu, X.; Feng, H.; Mawby, P.A. In Situ Contact Pressure Monitoring of Press Pack Power Module Using FBG Sensors. *IEEE Trans. Instrum. Meas.* **2022**, *71*, 1–11. [[CrossRef](#)]
91. Ren, H.; Ran, L.; Liu, X.; Liu, L.; Djurović, S.; Jiang, H.; Barnes, M.; Mawby, P. Quasi-distributed Temperature Detection of Press Pack IGBT Power Module Using FBG Sensing. *IEEE J. Emerg. Sel. Top. Power Electron.* **2021**, *10*, 4981–4992. [[CrossRef](#)]
92. Chen, S.; Vilchis-Rodriguez, D.; Djurović, S.; Barnes, M.; Mckeever, P.; Jia, C. Direct on Chip Thermal Measurement in IGBT Modules Using FBG Technology—Sensing Head Interfacing. *IEEE Sens. J.* **2022**, *22*, 1309–1320. [[CrossRef](#)]
93. Bazzo, J.P.; Lukasiewicz, T.; Vogt, M.; de Oliveira, V.; Kalinowski, H.J.; da Silva, J.C.C. Thermal characteristics analysis of an IGBT using a fiber Bragg grating. *Opt. Lasers Eng.* **2012**, *50*, 99–103. [[CrossRef](#)]
94. Jin-long, Z.; He, Y.; Jing, H.; Xiang-jun, X.; Feng, T. A Fiber Bragg Grating Sensing System for Monitoring IGBT Temperature Distribution and Thermal Conduction State of Upper Surface Silicone. In Proceedings of the Optical Sensing and Imaging Technologies and Applications, Beijing, China, 22–24 May 2018; p. 1084616. [[CrossRef](#)]
95. Chen, S.; Vilchis-Rodriguez, D.; Djurović, S.; Barnes, M.; Mckeever, P.; Jia, C. FBG Head Size Influence on Localized On-chip Thermal Measurement in IGBT Power Modules. *IEEE Sens. J.* **2022**, *22*, 1309–1320. [[CrossRef](#)]
96. De Moraes Sousa, K.; Probst, W.; Bortolotti, F.; Martelli, C.; Cardozo da Silva, J. Fiber Bragg Grating Temperature Sensors in a 6.5-MW Generator Exciter Bridge and the Development and Simulation of Its Thermal Model. *Sensors* **2014**, *14*, 16651–16663. [[CrossRef](#)]
97. João Paulo, B.; Tiago, L.; Marcio, V.; Mario, L.S.M.; Hypolito, J.K.; Jean, C.C.S. Performance Evaluation of an IGBT Module by Thermal Analysis Using Fiber Bragg Grating. In Proceedings of the Fourth European Workshop on Optical Fibre Sensors, Porto, Portugal, 8–10 September 2010; p. 76533Y. [[CrossRef](#)]